

Extremely fast vortex dynamics in $Bi_2Sr_2Ca_2Cu_3O_{10+\delta}$ crystalline nanostrip

A B Yu(于奥博), C T Lin(林成天), X F Zhang(张孝富), and L X You(尤立星)
Citation: Chin. Phys. B, 2023, 32 (**6**): 067402. DOI: 10.1088/1674-1056/acb425
Journal homepage: http://cpb.iphy.ac.cn; http://iopscience.iop.org/cpb

What follows is a list of articles you may be interested in

Photon number resolvability of multi-pixel superconducting nanowire single photon detectors using a single flux quantum circuit

Hou-Rong Zhou(周后荣), Kun-Jie Cheng(程昆杰), Jie Ren(任洁), Li-Xing You(尤立星),Li-Liang Ying(应利良), Xiao-Yan Yang(杨晓燕), Hao Li(李浩), and Zhen Wang(王镇)
Chin. Phys. B, 2022, 31 (**5**): 057401. DOI: 10.1088/1674-1056/ac398a

Investigation of dimensionality in superconducting NbN thin film samples with different thicknesses and NbTiN meander nanowire samples by measuring the upper critical field

Mudassar Nazir, Xiaoyan Yang(杨晓燕), Huanfang Tian(田焕芳), Pengtao Song(宋鹏涛), Zhan Wang(王战), Zhongcheng Xiang(相忠诚), Xueyi Guo(郭学仪), Yirong Jin(金贻荣), Lixing You(尤立星), Dongning Zheng(郑东宁)
Chin. Phys. B, 2020, 29 (**8**): 087401. DOI: 10.1088/1674-1056/ab9740

Fabrication of superconducting NbN meander nanowires by nano-imprint lithography

Mei Yang(杨美), Li-Hua Liu(刘丽华), Lu-Hui Ning(宁鲁慧), Yi-Rong Jin(金贻荣), Hui Deng(邓辉), Jie Li(李洁), Yang Li(李阳), Dong-Ning Zheng(郑东宁)
Chin. Phys. B, 2016, 25 (**1**): 017401. DOI: 10.1088/1674-1056/25/1/017401

Tunable coplanar waveguide resonator with nanowires

Zhou Yu (周渝), Jia Tao (郏涛), Zhai Ji-Quan (翟计全), Wang Cheng (汪橙), Zhong Xian-Qian (钟先茜), Cao Zhi-Min (曹志敏), Sun Guo-Zhu (孙国柱), Kang Lin (康琳), Wu Pei-Heng (吴培亨)
Chin. Phys. B, 2015, 24 (**4**): 047403. DOI: 10.1088/1674-1056/24/4/047403

Fabrication and properties of the meander nanowires based on ultra-thin Nb films

Zhao Lu (赵璐), Jin Yi-Rong (金贻荣), Li Jie (李洁), Deng Hui (邓辉), Zheng Dong-Ning (郑东宁)
Chin. Phys. B, 2014, 23 (**8**): 087402. DOI: 10.1088/1674-1056/23/8/087402

Extremely fast vortex dynamics in $Bi_2Sr_2Ca_2Cu_3O_{10+\delta}$ crystalline nanostrip

A B Yu(于奥博)[1,2,3], C T Lin(林成天)[4], X F Zhang(张孝富)[1,2,3,†], and L X You(尤立星)[1,2,3,‡]

[1] *State Key Laboratory of Functional Materials for Informatics, Shanghai Institute of Microsystem and Information Technology, Chinese Academy of Sciences, Shanghai* 200050, *China*

[2] *CAS Center for Excellence in Superconducting Electronics (CENSE), Shanghai* 200050, *China*

[3] *Center of Materials Science and Optoelectronics Engineering, University of Chinese Academy of Sciences, Beijing* 100049, *China*

[4] *Max Planck Institute for Solid State Research, Heisenbergstrasse* 1, *D*-70569 *Stuttgart, Germany*

(Received 15 November 2022; revised manuscript received 4 January 2023; accepted manuscript online 18 January 2023)

The maximum velocity of a mobile vortex in movement is generally limited by the phenomenon of flux-flow instability (FFI), which necessitates weak vortex pinning and fast heat removal from non-equilibrium electrons. We here demonstrate exfoliations and nano-fabrications of $Bi_2Sr_2Ca_2Cu_3O_{10+\delta}$ crystalline nanostrips, which possess a rather weak pinning volume of vortices, relatively low resistivity, and large normal electron diffusion coefficient. The deduced vortex velocity in $Bi_2Sr_2Ca_2Cu_3O_{10+\delta}$ crystalline nanostrips can be up to 300 km/s near the superconducting transition temperature, well above the speed of sound. The observed vortex velocity is an order of magnitude faster than that of conventional superconducting systems, representing a perfect platform for exploration of ultra-fast vortex matter and a good candidate for fabrications of superconducting nanowire single photon detectors or superconducting THz modulator.

Keywords: $Bi_2Sr_2Ca_2Cu_3O_{10+\delta}$ (Bi2223), vortices dynamics, ultra thin single crystal, nanowire

PACS: 74.72.–h, 47.32.cd **DOI:** 10.1088/1674-1056/acb425

1. Introduction

Dynamics of superconducting vortex at a bias current close to the depair critical current is of significant importance for both practical applications and insight into the fundamental physics of strongly interacting vortices.[1–7] For instance, in superconducting nanowire single-photon detectors (SNSPDs), to obtain high detection efficiencies, nanowires are commonly biased rather close to their experimental critical current. The single photon response process is thought of as vortices involved, either induced by vortices that overcome the suppressed edge barrier of nanowire by incident photons, or by the unbinding of thermally activated vortex–antivortex pairs in the suppressed hotspot region caused by incident photons.[8–11] Such fast-moving vortices in superconducting nanowires may in part explain the extraordinary timing resolution property of SNSPDs. Moreover, for a type-Ⅱ superconducting flux flow oscillator (FFO), it has been found that in the vortex flux flow regime, when vortex emerges the surface periodically with a frequency of v/a,[7] a THz radiation with harmonics of this frequency up to the superconducting gap will be emitted,[12] where v is the vortex velocity and $a = \left(2\phi_0/\sqrt{3}B\right)^{0.5}$ is the inter-vortex distance with an assumed triangular vortex lattice. With respect to the physics of fast-vortex involved non-equilibrium superconducting system, despite the physics of quasi-static vortices lattice or glass has been thoroughly investigated, fundamental physics concerning the superfast vortices in the flux-flow state still remains complicated, which evokes much attention both experimentally and theoretically.[13–18]

Fundamentally, the maximal current that superconductors can carry is the depairing current, which is determined by the critical velocity of Cooper pairs.[19,20] However, the maximal applicable current of superconductors in magnetic field is associated with the de-pinning of vortex and the subsequent FFI. Vortices, as dual particles to Cooper pairs, can be activated and delocalized by excess bias current and magnetic field. The subsequent vortex motion results in finite voltage drops along the superconductor and form a resistive state where the following current is sufficiently smaller than $I_{\rm dep}$, in which the global coherence of superconductivity is broken down.[20] The maximal non-dissipation current $I_{\rm c}$ of the immobile vortex state is commonly 10%–30% lower than $I_{\rm dep}$. Beyond $I_{\rm c}$ in the flux-flow regime, vortices, which are accelerated by the Lorentz force $F_{\rm L} = I_{\rm b} \times \hat{\phi}_0$ with $I_{\rm b}$ being the bias current and $\hat{\phi}_0$ the flux quantum, can move with high velocity v,[20,21] and eventually leads to a quench of the superconducting state at I^* as a consequence of vortex instability (flux-flow instability, FFI), resulting in a sudden voltage jump in the current-voltage curves.[6,7,22–26] The maximal vortex velocity is therefore associated with the FFI phenomena. Researchers have demonstrated vortex velocities of a few km/s in traditional

†Corresponding author. E-mail: zhangxf@mail.sim.ac.cn

‡Corresponding author. E-mail: lxyou@mail.sim.ac.cn

© 2023 Chinese Physical Society and IOP Publishing Ltd

disordered and amorphous superconducting thin films,[27–30] and slightly faster vortex dynamics in unconventional high T_c thick films.[31,32] Ultra-fast vortex velocities up to more than 10 km/s, however, are recently observed in a directly written NbC superconductor with a close-to-perfect edge barrier,[6] a 15-nm-thick amorphous MoSi focused ion beam (FIB) milled bridges,[33] and has also been directly probed by a scanning superconducting quantum interference device microscopy in lead microbridge.[7] Such a high velocity of vortex is well beyond the speed of sounds, which is of great significance for magnetic flux transport via superconducting vortices and the phenomena of generation of sound and spin waves by moving fluxons.[34,35]

Based on these previous investigations, a high T_c superconducting microbridge with good bridge-edge would be an optimal platform for accessing extremely fast vortex dynamics.[36] To this end, we here fabricated $Bi_2Sr_2Ca_2Cu_3O_{10+\delta}$ (Bi2223) nanostrips by direct laser writing to avoid possible degradations from electron beam lithography, and milling by an Ar ion beam. The normal resistivity of the resulting nanostrip is around 220 $\mu\Omega\cdot$cm ($T = 120$ K), and the vortex velocities deduced from the current–voltage (I–V) characteristics can be up to three hundreds of kilometers per second.

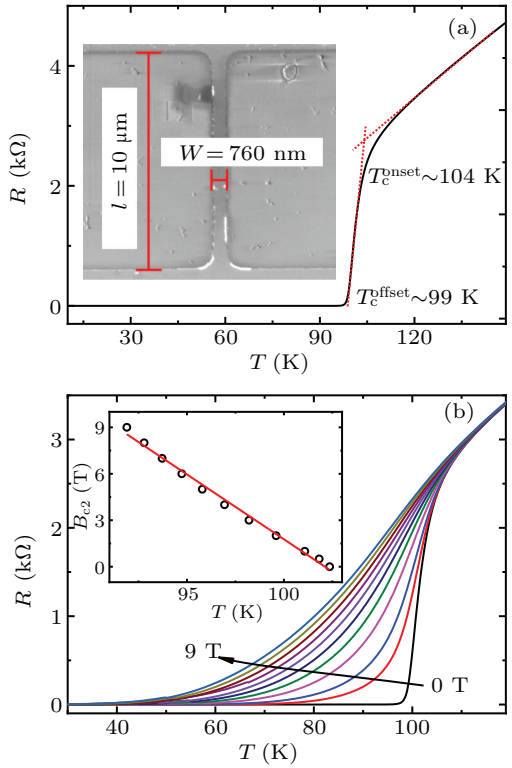


Fig. 1. (a) Zero-field normal to superconducting transitions of the Bi2223 crystalline nanostrip. Inset: scanning electron microscope image of the nanostrip. (b) Field-dependent normal to superconducting transitions of the nanostrip from 0 to 9 T. Inset: the extracted upper critical field as a function of magnetic field.

2. Experiment

A three-unit-cell (3 U.C.) thick (confirmed by the atomic force microscope scanning) Bi2223 crystalline flake was firstly exfoliated from a bulk crystal, which was synthesized by using a travelling solvent floating zone method.[37,38] To avoid possible irradiation defects induced by high energy electron beam lithography, we here adopted the laser direct-writing technique to fabricate the superconducting nanostrip. Although the oxygen atoms of ultra-thin Bi-based high T_c superconductor are prone to degrade even under ambient conditions when reduce the thickness down to 0.5 U.C.,[39] and cryogenic cleavage is necessitated for ultra-thin Bi-based high T_c superconductor in constructing twisted cuprate superconductors.[40] However, recent experiments[36,41] showed that thin flakes of Bi-based high T_c superconductor exfoliated at room temperature still maintain relatively high T_c for films with thickness more than 2 U.C. if the exposure time to ambient environment is limited within 20 min. We here fabricated two different Bi2223 bridges with thicknesses of 3 U.C and 2.5 U.C, respectively. The detailed fabrication process of Bi2223 sub-microbridge is described elsewhere.[36] As shown in Fig. S1 of the supplementary material, characteristic curves of resistance and current versus voltage are measured by a standard four-wire method by using a resistance bridge and electrical transport options of physical property measurement system (PPMS, Quantum Design). The contact resistance has few influences on the measurements of current–voltage characteristics and it is discussed in Fig. S2.

3. Results and discussion

As shown in the inset in Fig. 1(a), the length and width of the nanostrip are 10 μm and 760 nm, respectively. The main plot of Fig. 1(a) displays the temperature dependence of the resistance $R(T)$ for the fabricated Bi2223 nanostrip. The $R(T)$ in the normal state shows a metallic-like character, and it deviates from the metallic-like behavior around 115 K, similar to the bulk Bi2223 crystal.[36] The zero-field superconducting onset (T_c^{onset}) and offset (T_c^{offset}) temperature are evaluated to be 104 K and 99 K, respectively. The field-dependent normal to superconducting transitions from 0 T to 9 T were measured at temperatures from 10 K to 120 K, as shown in the main plot of Fig. 1(b). The smooth superconducting transitions at all fields suggest that the fabricated nanostrip is reasonably homogeneous and of good quality. The field-dependent superconducting transition T_c is defined as the temperature where $R(T)$ falls to half the normal state resistivity at $T = 120$ K, which are summarized in the inset of Fig. 1(b). Near T_c, by linearly fitting to the temperature dependence of the upper critical

field $B_{c2}(T)$, the slope is found to be $dB_{c2}/dT \cong -0.84$ T/K, corresponding to a diffusion coefficient of the normal state electrons of $D = -1.097\,(dB_{c2}/dT)^{-1} = 1.3$ cm^2/s, which is far larger than traditional disordered superconductors.[42] The zero-temperature critical field is commonly derived from the slope of the determined by $B_{c2}(0) = -0.73 \times (dB_{c2}/dT)\,T_c \cong 62.5$ T in the clean limit.[43] The zero-temperature Ginzburg Landau (GL) coherence length can then be estimated to be $\xi(0) = \sqrt{\phi_0/2\pi B_{c2}(0)} = 2.3$ nm.

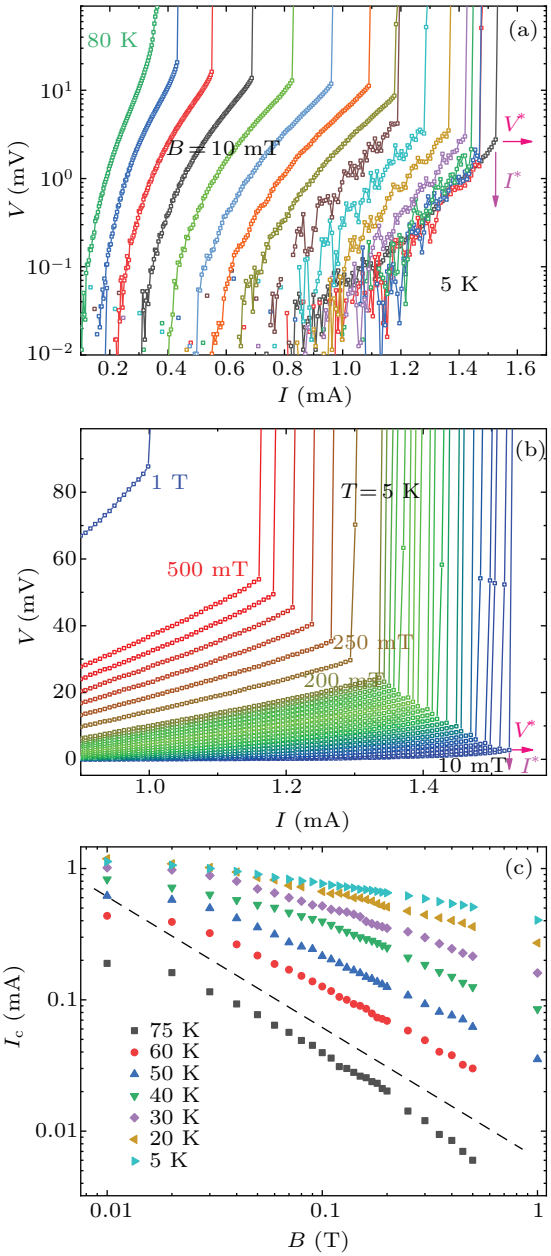


Fig. 2. (a) The *I*–*V* curves of the nanostrip at temperatures from 5 K to 80 K in a magnetic field of 10 mT. The definition of the instability current I^* and the instability voltage V^* are illustratively marked. (b) *I*–*V* curves of the nanostrip in a series of magnetic fields from 10 mT to 1 T at 5 K. (c) Critical current as a function of magnetic fields at temperatures from 5 K to 75 K. The dashed line schematically shows a B^{-1} dependence.

The current–voltage (*I*–*V*) characteristics as a function of applied fields were measured from 80 K to 5 K. In Figs. 2(a) and 2(b) we show the temperature-dependent *I*–*V* curves at $B = 10$ mT and typical field-dependent *I*–*V* curves at $T = 5$ K, respectively, in which well-defined voltage jumps are observed at the critical point marked by (I^*, V^*). In addition, the full-range *I*–*V* curves is displayed in Fig. S3 of the supplementary material. These *I*–*V* curves can be distinctly classified into three different regimes: zero-resistivity superconducting regime, finite-resistivity flux-flow regime, and the FFI regime. To avoid the overheating induced breakdown of the Bi2223 nanostrip, we have set a voltage limit of 130 mV on the nanostrip. As a result, an Ohmic normal state *I*–*V* dependence is absent on the recorded *I*–*V* curves.

The non-dissipation critical current I_c is then uniformly determined by a 100 μV voltage criterion, and the field dependence for several selected temperatures are summarized in Fig. 2(c). The experimental $I_c(B)$ dependences decrease nonlinearly at all temperatures, showing a $B^{-\alpha}$ dependence. Near T_c^{offset}, $I_c(B)$ can be well described by a B^{-1} dependence, suggesting an edge barrier for vortex entry dominated mechanism in the Bi2223 nanostrips,[6] as shown in Fig. 2(c). As mentioned above, when bias current I_b is less than the depinning current, the pinning force F_p is larger than Lorentz force F_L of vortices, and the superconductors are in zero-resistivity superconducting regime. The F_L of vortices will increase with the increasing I_b, and vortices can move when $F_L > F_p$. At this time, the superconductors are pulled to flux-flow regime. When I_b reaches I^*, a sudden jump of voltage to normal state appears, suggesting flux flow instability. According to Refs. [6,44], the relationship between critical voltage point V^* and the maximal vortex instability velocity v^* is given by the equation $V^* = v^* Bl$, where $l = 10$ μm is the length of the nanostrips. Hence, we can deduce the values of v^*. The field-dependent $v^*(B)$'s are summarized in Fig. 3(a) for all investigated temperatures, which are found to decrease with the increase of B. For example, at 75 K, the resulting v^* at 10 mT can reach as fast as 208 km/s, while it decreases to 18 km/s at 0.5 T, which remains substantially constant in the relatively high field limit.

To account for the ultra-fast vortex dynamics observed in our clean Bi2223 nanostrips, the underlying ideas that suppresses the FFI are of great importance. Generally, for mobile vortices, their associated electric field raises the energy of quasiparticles inside the vortex core, which in turn leads to the leakage of quasiparticles from the core of vortices. As a result, the vortex core shrinks and the viscous friction on vortex reduces. The velocity of vortices is therefore further accelerated, which eventually gives rise to the collapse of flux-flow state and a quenching to the normal resistive state.[22,45] According

to the Larkin–Ovchinnikov (LO) FFI model, which is considered for a highly disordered superconductor near T_c (in which the electron–electron interaction time τ_{ee} is far smaller than the electron–phonon interaction time), the maximal vortex velocity v^* is related with the normal electron diffusion coefficient and the quasiparticle relaxation time τ_ε.[22,45] Namely, superconducting systems with larger diffusion coefficient of the normal state electrons and shorter τ_ε would benefit the realization of ultra-fast vortex dynamics. For instance, ultra-fast vortex velocities beyond the speed of sound were recently probed in a Nb-C superconductor with a fast relaxation time of quasiparticles and in a lead microbridge with a large diffusion coefficient and a short inelastic electron–phonon relaxation time.[6,7]

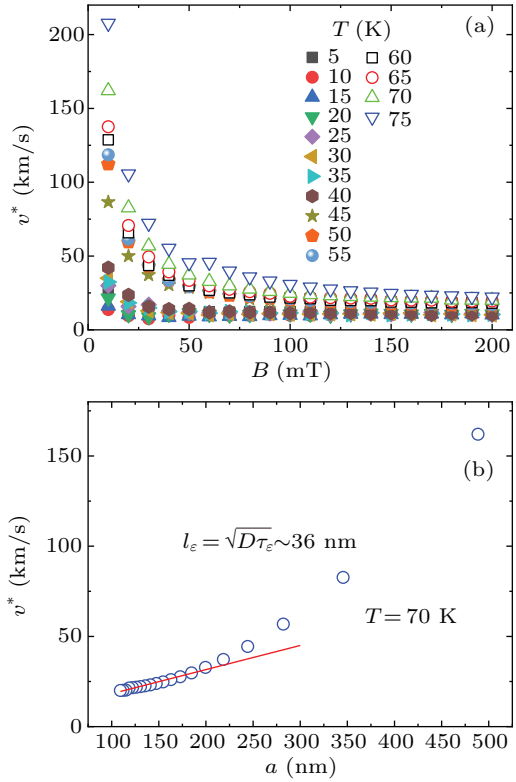


Fig. 3. (a) The instability velocity v^* as a function of magnetic fields at temperatures from 5 K to 75 K. (b) The instability velocity v^* as a function of the intervortex distance. The red solid line is a fit to the Doettinger modified FFI model.

The LO-FFI model, which neglects the heating effects from the Joule dissipation of nonequilibrium quasiparticles, was further extended by Bezuglyj and Shklovskij[23] that took the Joule heating into account, and by Doettinger *et al.*[46] that took the magnetic field dependence of the vortex lattice parameter into account. From the LO model modified by Doettinger *et al.*, the quasiparticle energy relaxation time can be deduced from a fitting to

$$v^* = \left(\frac{4.1\,(1-T/T_c)^{1/2}D}{\pi\tau_\varepsilon}\right)^{1/2}\left(1+\frac{a}{\sqrt{D\tau_\varepsilon}}\right). \quad (1)$$

As shown in Fig. 3(b), we present a critical velocity dependence on intervortex distance, yielding a quasiparticle diffusion length of $l_\varepsilon = \sqrt{D\tau_\varepsilon} \sim 36$ nm, which is far smaller than the intervortex distance at the involved fields and in turn maximally minimize the viscous friction force on vortex. From the diffusion coefficient, the energy relaxation time is therefore estimated to be $\tau_\varepsilon \sim 10$ ps, which is nearly two orders of magnitude smaller than that from a sputtering deposited thick $Bi_2Sr_2CaCu_2O_{8+\delta}$ bridges.[32] It is also interesting to note that the non-equilibrium quasi-particle relaxation time in clean high T_c superconductors (measured by pump-probe optical spectroscopy) at T_c can even be in the sub-ps range.[47] The superconducting system with fast quasiparticle energy relaxation time is essential for high velocity of vortices, since a short τ_ε is able to rapidly cool down the leaked heating quasiparticles on the vortex path. However, these FFI models are based on those highly disordered superconductors, and further sophisticated investigation based on the time-dependent GL simulation would reveal more underlying physics for the Bi2223 crystalline nanostrips.

To further verify the ultra-fast vortices dynamics in Bi-2223 nanostrips, we here also fabricated a slightly thinner Bi-2223 nanostrip (2.5 U.C.) with a similar strip width (900 nm). As it is shown in Fig. 4(a), the 2.5 U.C. nanostrip shows a slightly reduced T_c^{onset}, around 102 K. The zero-resistivity critical temperature T_{c0}, however, is suppressed below 80 K, which may be attributed to degradations during the etching process and exposure to air. We also systematically investigate the current-voltage characteristics of the 2.5 U.C. nanostrip near T_{c0}. The deduced v^* as a function of field for temperatures of 70 K and 72 K are shown in Fig. 4(b). An even faster vortex velocity is observed in this thinner nanostrip, which can be as fast as 316 km/s in the low field limit. In thinner superconducting films, the τ_ε is smaller than that in thicker films, as observed in NbN films.[44] The larger critical velocity observed in a 2.5 U.C device may be ascribed to the shorter τ_ε in thinner nanostrips.

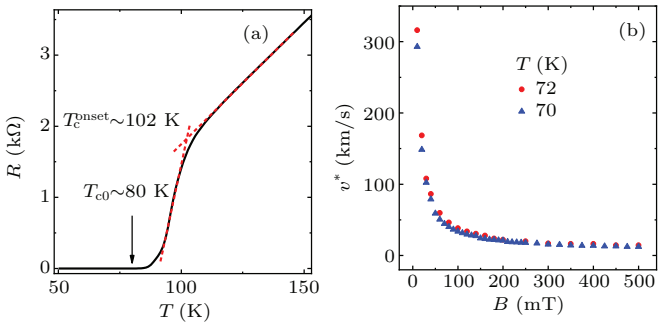


Fig. 4. (a) Zero-field normal to superconducting transitions of a 2.5 U.C. Bi2223 crystalline nanostrip. (b) The instability velocity v^* as a function of magnetic fields near T_{c0}.

However, with the increasing bias current, the normal current may also appear, leading to a component of voltage drop. Generally, the normal state electrons that induce normal current would result in a contribution to the voltage drop. Basically, there would be three components of normal electrons: (a) the normal electron inside the vortex core; (b) in the quasi-two-dimensional limit, under high flux flow speed, the shape of the vortex would shrink and normal electrons would escape from the normal core; (c) thermally activated non-equilibrium quasi-particles. For the contribution (a), it is the main contribution that induces the flux-flow instability. For the contributions of (b) and (c), we are unable to make an exact calculation about the portion to the total contribution of the voltage drop. Nevertheless, as we estimated in the manuscript, a short τ_ε of our exfoliated Bi2223 crystal is able to rapidly cool down the leaked non-equilibrium quasiparticles. Such contributions from the non-electrons or non-equilibrium quasiparticles are therefore not considered in this manuscript.

Finally, it is worthy to note that pronounced hysteresis characteristics are observed these I–V curves at relatively low temperatures, due to the bias current generated Joule heating in the normal state and the self-recovery process (Fig. S4 in the supplementary material). Such a metastable state in superconducting nanowire or microwire is necessary for generations of voltage pulses upon photon absorptions. For instance, a switching current of $I_{SW} = 1.54$ mA and a retrapping current $I_r = 0.61$ mA is observed for the 3 U.C. nanostrip. While it has been predicted that single telecom photon induced hotspot would be an order of magnitude smaller than that in conventional superconducting NbN nanowires, single photon detections are recently successfully observed in 100 nm wide and 10–15 nm thick Bi-2212 nanowires,[48] or in a $\gtrsim 15$ nm thick and 250 nm wide Bi-2212 nanowires.[49] Although the relatively large normal electron diffusion coefficient smear the hotspot and lower the effective temperature inside it, the extremely small coherence length and low carrier density would enhance the impact of photon absorption on the suppression of superconductivity in narrow Bi-2223 nanowires. These results suggest that the narrow Bi-2223 nanowires would also be good candidates for fabrications of SNSPDs.

4. Conclusion

To summarize, we have successfully fabricated a few-U.C.-thick high-T_c superconducting Bi2223 nanostrips by direct laser writing technique. The fabricated Bi2223 nanostrips show onset critical temperatures above 100 K, and zero-resistivity critical temperature far above the liquid nitrogen temperature. We have experimentally observed ultra-fast vortex dynamics with velocities up to 300 km/s, which is the fastest vortex velocities reported to date. Such fast vortex velocities in Bi2223 nanostrips are attributed to combined effects from the good structural and superconducting homogeneity, huge bias current excited Lorentz force, and short quasiparticles relaxation time induced fast heat removal from leaked quasiparticles. Such a few-U.C.-thick Bi2223 flakes are therefore perfect platforms for research of far-from-equilibrium superconductivity and fast vortex associated physics, and applications for THz radiation modulators or emitters. Moreover, due to the large critical current, high superconducting transition temperature and fast quasiparticles relaxation time, the crystalline Bi2223 nanowires would also be good candidates for fabrications of SNSPDs with high count rates and low timing jitter.

Acknowledgements

The authors are grateful to Y. Y. Wang for supporting high quality of post growth treatment $Bi_2Sr_2Ca_2Cu_3O_{10+\delta}$ single crystals. This study was supported by the National Key Research and Development Program of China (Grant No. 2017YFA0304000), the National Natural Science Foundation of China (Grant Nos. 61971408 and 61827823), Shanghai Municipal Science and Technology Major Project (Grant No. 2019SHZDZX01), Shanghai Rising-Star Program (Grant No. 20QA1410900), the Youth Innovation Promotion Association of Chinese Academy of Sciences (Grant Nos. 2020241 and 2021230), and the Natural Science Foundation of Shanghai (Grant No. 19ZR1467400). The experimental measurements were supported by the Superconducting Electronics Facility (SELF) of Shanghai Institute of Microsystem and Information Technology.

References

[1] Rouco V, Navau C, Del-Valle N, *et al.* 2019 *Nano Lett.* **19** 4174
[2] Veshchunov I S, Magrini W, Mironov S V, *et al.* 2016 *Nat. Commun.* **7** 12801
[3] Kremen A, Wissberg S, Haham N, *et al.* 2016 *Nano Lett.* **16** 1626
[4] Lara A, Aliev F G, Moshchalkov V V, *et al.* 2017 *Phys. Rev. Appl.* **8** 034027
[5] Grimaldi G, Leo A, Sabatino P, *et al.* 2015 *Phys. Rev. B* **92** 024513
[6] Dobrovolskiy O V, Vodolazov D Y, Porrati F, *et al.* 2020 *Nat. Commun.* **11** 3291
[7] Embon L, Anahory Y, Jelic Z L, *et al.* 2017 *Nat. Commun.* **8** 85
[8] Zotova A N and Vodolazov D Y 2012 *Phys. Rev. B* **85** 024509
[9] Vodolazov D Y, Korneeva Y P, Semenov A V, *et al.* 2015 *Phys. Rev. B* **92** 104503
[10] Vodolazov D Y 2017 *Phys. Rev. Appl.* **7** 034014
[11] Bulaevskii L N, Graf M J and Kogan V G 2012 *Phys. Rev. B* **85** 014505
[12] Sarreshtedari F, Hosseini M, Chalabi H R, *et al.* 2009 *IEEE Trans. Appl. Supercond.* **19** 3653
[13] Vodolazov D Y and Peeters F M 2007 *Phys. Rev. B* **76** 014521
[14] Gurevich A and Ciovati G 2008 *Phys. Rev. B* **77** 104501
[15] Kogan V G and Prozorov R 2020 *Phys. Rev. B* **102** 024506

[16] Pathirana W and Gurevich A 2020 *Phys. Rev. B* **101** 064504
[17] Kogan V G and Nakagawa N 2021 *Phys. Rev. B* **103** 134511
[18] Pathirana W and Gurevich A 2021 *Phys. Rev. B* **103** 184518
[19] Vodolazov D Y 2014 *Phys. Rev. B* **90** 054515
[20] Blatter G, Feigel'man M V, Geshkenbein V B, *et al.* 1994 *Rev. Mod. Phys.* **66** 1125
[21] Thomann A U, Geshkenbein V B and Blatter G 2012 *Phys. Rev. Lett.* **108** 217001
[22] Larkin A I and Ovchinnikov Y N 1986 *Nonequilibrium Superconductivity* (North-Holland: Elsevier) p. 711
[23] Bezuglyj A I and Shklovskij V A 1992 *Physica C* **202** 234
[24] Vodolazov D Y. 2019 *Supercond. Sci. Technol.* **32** 115013
[25] Dobrovolskiy O V, Gonzalez-Ruano C, Lara A, *et al.* 2020 *Commun. Phys.* **3** 64
[26] Leo A, Nigro A and Grimaldi G 2020 *Low Temp. Phys.* **46** 375
[27] Liu Z, Luo B, Zhang L, *et al.* 2021 *Supercond. Sci. Technol.* **34** 125014
[28] Hofer J A and Haberkorn N 2021 *Thin Solid Films* **730** 138690
[29] Cirillo C, Granata V, Spuri A, *et al.* 2021 *Phys. Rev. Mater.* **5** 085004
[30] Lin S Z, Ayala-Valenzuela O, McDonald R D, *et al.* 2013 *Phys. Rev. B* **87** 184507
[31] Xiao Z L and Ziemann P 1996 *Phys. Rev. B* **53** 15265
[32] Xiao Z L, Voss-de Haan P, Jakob G, *et al.* 1998 *Phys. Rev. B* **57** R736
[33] Budinska B, Aichner B, Vodolazov D Y, *et al.* 2022 *Phys. Rev. Appl.* **17** 034072
[34] Golovchanskiy I A, Abramov N N, Stolyarov V S, *et al.* 2018 *Adv. Funct. Mater.* **28** 1802375
[35] Dobrovolskiy O V, Sachser R, Bracher T, *et al.* 2019 *Nat. Phys.* **15** 477
[36] Yu A B, Huang Z, Peng W, *et al.* 2022 *Appl. Phys. Lett.* **120** 072601
[37] Liang B, Bernhard C, Wolf T, *et al.* 2004 *Supercond. Sci. Technol.* **17** 731
[38] Lin C T and Liang B 2002 *New Trends in Superconductivity* (Berlin: Springer) pp. 19–28
[39] Yu Y, Ma L, Cai P, *et al.* 2019 *Nature* **575** 156
[40] Zhao S Y F, Poccia N, Cui X, *et al.* 2021 arXiv:2108.13455 [cond-mat.supr-con]
[41] Wang T, Yu A, Liu Y, *et al.* 2022 *Phys. Rev. B* **106** 104509
[42] Zhang X, Engel A, Wang Q, *et al.* 2016 *Phys. Rev. B* **94** 174509
[43] Helfand E and Werthamer N R 1964 *Phys. Rev. Lett.* **13** 686
[44] Zhang L, You L, Peng W, *et al.* 2020 *Physica C* **579** 1353773
[45] Larkin A I and Ovchinnikov Y U N 1975 *Sov. Phys. JETP* **41** 960
[46] Doettinger S G, Huebener R P and Kuhle A 1995 *Physica C* **251** 285
[47] Hunt C R, Nicoletti D, Kaiser S, *et al.* 2016 *Phys. Rev. B* **94** 224303
[48] Charaev I, Bandurin D A, Bollinger A T, *et al.* 2023 *Nat. Nanotechnol.* **18** 343
[49] Merino R L, Seifert P, Retamal J D, *et al.* 2022 arXiv:2208.05044 [cond-mat.supr-con]